

## 음향방사력을 이용한 효모세포의 크기별 분리

라이한 하디 줄리오\* · 무함마드 소반 칸\* · 무스타크 알리\* · 굴람 데스트기르\*\* · 박진수\*,†

### Size-based Separation of Yeast Cell by Surface Acoustic Wave-induced Acoustic Radiation Force

Raihan Hadi Julio\*, Muhammad Soban Khan\*, Mushtaq Ali\*, Ghulam Destgeer\*\*, and Jinsoo Park\*,†

**Abstract** The yeast *Saccharomyces cerevisiae* (*S. cerevisiae*) is considered an ideal eukaryotic model and has long been recognized for its pivotal role in numerous industrial production processes. Depending on the cell cycle phases, microenvironment, and species, *S. cerevisiae* varies in shape and has different sizes of each shape such as singlets, doublets, and clusters. Obtaining high-purity populations of uniformly shaped *S. cerevisiae* cells is crucial in fundamental biological research and industrial operations. In this study, we propose an acoustofluidic method for separating *S. cerevisiae* cells based on their size using surface acoustic wave (SAW)-induced acoustic radiation force (ARF). The SAW-induced ARF increased with cell diameter, which enabled a successful size-based separation of *S. cerevisiae* cells using an acoustofluidics device. We anticipate that the proposed acoustofluidics approach for yeast cell separation will provide new opportunities in industrial applications.

**Key Words** : Surface Acoustic Wave (표면탄성파), Acoustofluidics (음향미세유체역학), Acoustic Radiation Force (음향방사력), Yeast Cell (효모 세포)

### 1. Introduction

Yeast *Saccharomyces cerevisiae* (*S. cerevisiae*) is a versatile species with a wide range of applications in various fields including molecular biology, biotechnology, and food production<sup>(1,2)</sup>. In general, due to their ease of manipulation, *S.*

*cerevisiae* cells have become a crucial tool for understanding the recombination and transmission of genetic material in scientific research<sup>(3)</sup>. Their rapid growth and easy cultivation provide an abundant supply of cells for experimentation. Yeast cells are composed of various chemical components such as proteins, carbohydrates, minerals, ribonucleic acid, and lipids, which lead to the importance of this cell in the genomic field<sup>(4)</sup>. Furthermore, yeast cells exhibit typical eukaryotic characteristics, which enables genomic manipulation, making it possible to use yeast cells as a model

---

† Correspondence to Jinsoo Park  
E-mail: jinsoopark@jnu.ac.kr

\* Department of Mechanical Engineering,  
Chonnam National University, Republic of Korea

\*\* Department of Electrical Engineering,  
Technical University of Munich, Germany

---

for studying human cells<sup>(5)</sup>. *S. cerevisiae* has different shapes such as singlets, doublets, and clusters depending on the cell cycle phases, microenvironment, and species.

Accurate separation of cells with high purity from complex and heterogeneous mixtures is essential in numerous biological, biotechnological, and medical applications<sup>(6)</sup>. The cell separation phenomena are associated with size, density, compressibility, and other intrinsic properties of the cells and suspension. Adherence to a solid surface, density gradients in a centrifuge tube, and binding of to specific antibody-coated surfaces have been demonstrated as traditional techniques for decades to separate cells of interest<sup>(7)</sup>. Lab-on-a-chip gives a new and modern approach, replacing the traditional cell separation techniques. A lab-on-a-chip integrates diverse microfluidic technologies by miniaturizing bulky and numerous components into a compact chip. Microfluidics platform offers several advantages including a low consumption of samples, cost-effective operation and production, and integration of various heterogeneous pre- and post-separation functions. Numerous microfluidic methods have been employed to separate microparticles that are of a similar size to cells. Among these methods, acoustofluidics stands out as it enables label-free and continuous separation. Previous studies showed that yeast cell separation has been successfully demonstrated in microfluidic chips using active<sup>(8)</sup> and passive<sup>(9)</sup> methods. Ping *et al.*<sup>(6)</sup> utilized a passive microfluidic technique for yeast *S. cerevisiae* separation by shape using viscoelastic and Newtonian fluids. Furthermore, Eliezer *et al.*<sup>(10)</sup> utilized an inertial microfluidics platform to isolate large quantities of young and adult yeast cells from a mixed population. These passive methods rely on the fluid properties and precise flow rate control to effectively separate the cells. In addition, passive microfluidic approaches require a

specific geometry of the channel because of the strong dependency on hydrodynamic forces. Honeyeh and Christian<sup>(11)</sup> demonstrated the separation of live and dead yeast cells using a dielectrophoresis technique by tuning the crossover frequency that strongly depends on the electrical properties of the cells and media.

In this research, we introduce an acoustofluidic technique for the separation of *S. cerevisiae* cells based on their sizes using traveling surface acoustic wave (TSAW)-induced acoustic radiation force (ARF). A cross-type microfluidic device was used, such that TSAWs travel perpendicular to the flow direction within the fluid medium, interacting with *S. cerevisiae* cells and thus inducing ARF. Variations in the magnitude of TSAW-induced ARF acting on cells of different sizes allowed us to successfully separate *S. cerevisiae* cells based on size. Previously, we demonstrated the separation of Tardigrades (100 $\mu\text{m}$  in length) from their eggs and algal food in a raw sample by using TSAW-ARF. This is the first report of separating living organisms by direct ARF by TSAW with diameters  $< 15 \mu\text{m}$ <sup>(12)</sup>.

## 2. Methodology

Fig. 1 shows the schematic diagram of the cross-type microfluidic device employed in this work. The device comprises a slanted finger interdigital transducer (SFIT) composed of a metallic bilayer

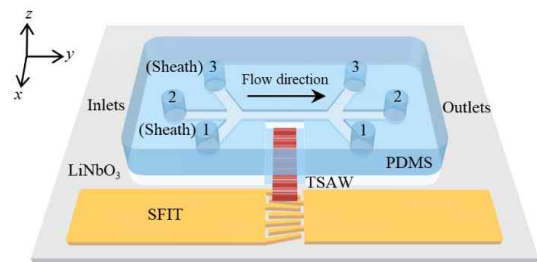


**Fig. 1.** Perspective view of proposed microfluidic devices used in this research.

(Cr and Au) deposited on a piezoelectric lithium niobate (LN) substrate (128° Y-X cut, 0.5-mm thick, 4-inch diameter, MTI Korea). A polydimethylsiloxane (PDMS) microchannel was affixed on the LN substrate adjacent to the SFIT such that acoustic waves generated from the transducer are perpendicular to the fluid flow direction. Two SFITs have finger spacing ( $\lambda/4$ ) of 8.5-13  $\mu\text{m}$  and 6.5-8.5  $\mu\text{m}$  that corresponds to a frequency range of 70-115 MHz and 116-152 MHz, respectively. Each SFIT has 40 finger pairs with a total aperture of 1000  $\mu\text{m}$ . The active frequencies actuated at the first and second SFIT were 100 and 141 MHz, respectively. The soft lithography technique was employed for the fabrication of the PDMS microchannel, which was then securely attached to the LN substrate using oxygen plasma bonding (Covance, Femto Science). The height of the microchannel was 50  $\mu\text{m}$  whereas the width of the main acoustic actuation region was 500  $\mu\text{m}$ . PDMS microchannel consists of three inlets and three outlets. Inlets 1 and 3 were utilized for injecting sheath fluids i.e., DI water. On the other hand, inlet 2 was utilized to inject sample fluid carrying yeast cells (YSC1-100G, Sigma-Aldrich). The sheath fluids hydrodynamically focused the suspended yeast cells close to the bottom microchannel wall, nearest to the SFITs. In addition, the purpose of sheath fluids is to avoid the microchannel anechoic corner (MAC), a region with a weak acoustic field, formed within the channel corner due to oblique propagation of leaky TSAW at the Rayleigh angle<sup>(13,14)</sup>. Fluids were injected into the microchannels using a high-precision multi-syringe pump (neMESYS Cetoni GmbH).

Upon applying the AC voltage across the terminal of the SFIT, acoustic waves were generated on the LN substrate<sup>(15)</sup>. The TSAW emanated from the electrodes and proceeded towards the PDMS microchannel, where they encountered the flowing fluid. The Rayleigh-type

TSAWs were then transmitted into the fluid medium within the microchannel in the form of longitudinal waves. When a solid micro-object or spherical particle suspended in a liquid intercepted the acoustic field, an inhomogeneous wave scattering occurred at the interface between the solid and liquid due to differences in acoustic impedance. This acoustic interaction led to the generation of TSAW-induced ARF acting on the microparticles predominantly in the direction of wave propagation<sup>(16)</sup>. The ARF exerted on the object was dependent on microparticle diameter, TSAW frequency, and relative density and compressibility of suspension media with respect to the object. The radiation force acting on the microparticle can be estimated using the ARF factor ( $F_F$ ). The  $F_F$  is a dimensionless parameter that represents the force applied to a microparticle per unit acoustic energy density per unit cross-sectional area of the particle. The  $F_F$  induced by TSAW acting on an elastic particle are approximated using elastic sphere theory<sup>(17)</sup>:

$$F_F = \langle \text{ARF} \rangle / (\pi d_p^2 \bar{E} / 4) \quad (1)$$

where  $\langle \text{ARF} \rangle$ ,  $d_p$  and  $\bar{E}$ , represent time-averaged acoustic radiation force, microsphere diameter, and mean energy density. The dominance of the ARF acting on microparticles in a fluid medium is generally estimated using the dimensionless number known as the Helmholtz number ( $\kappa$ ). This dimensionless number is dependent on the size of the microsphere as well as the acoustic wavelength and can be expressed as:

$$\kappa = \frac{\pi d_p}{\lambda_f} \quad (2)$$

where  $\lambda_f$  is the acoustic wavelength in the fluid. Upon application of the acoustic wave on the

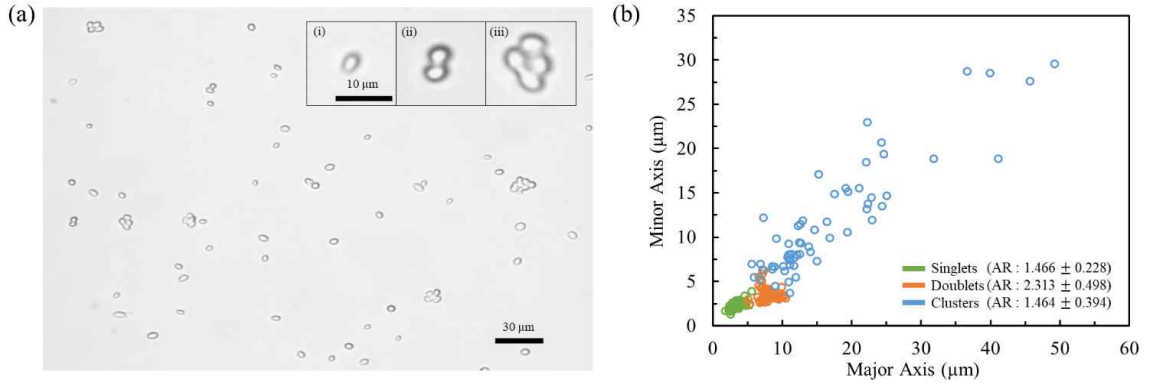


**Fig. 2.** (a) Observed microscopy image of *S. cerevisiae* showing singlets (i), doublets (ii), and clusters (iii); (b) Scatters plot of *S. cerevisiae* cell size.

microparticle traveling within the fluid, the acoustic wave scattered off the microparticle. For  $\kappa \approx 1$ , the scattering off a solid elastic microsphere was noted within the Mie scattering regime. On the contrary, when  $\kappa \gg 1$  the acoustic wave scattering off the microparticle occurred in the Geometric scattering regime. Mie scattering is observed when the size of the object is of a similar magnitude to the wavelength, while in geometrical scattering, the object size greatly exceeds the wavelength, resulting in an enhanced magnitude of  $ARF^{(18)}$ .

Fig. 2(a) shows the observed microscopic image of *S. cerevisiae* utilized in the study along with insets displaying the shapes of singlets (i), doublets (ii), and clusters (iii). The average effective diameter of singlets, doublets, and clusters was 2.7, 4.6, and 13.1 μm, respectively. Furthermore, the size distribution of singlets, doublets, and clusters have been plotted against their major and minor axis as depicted in Fig. 2(b). As can be seen in the results that *S. cerevisiae* cells exhibited a distinct shape with the ratio of major to minor axis (aspect ratio, AR). The AR of singlets, doublets, and clusters were found to be  $1.466 \pm 0.228$ ,  $2.313 \pm 0.498$ , and  $1.464 \pm 0.394$ . The comprehensive examination of size and shape parameters is essential for understanding the behavior of these cells upon experiencing

TSAW-induced ARF.

Fig. 3 shows the numerical calculation of  $F_F$  with varying  $f$  and the diameter of the *S. cerevisiae* cells. The response of the *S. cerevisiae* cells to SAW-induced ARF is notably stronger at specific frequencies, primarily because of the free vibration of *S. cerevisiae* cells. The frequencies suitable for effectively manipulating *S. cerevisiae* cells are mainly dictated by their size, compressibility, and density. In this study, a two-step separation has been conducted to separate singlets, doublets, and clusters with high purity. The first separation was performed to distinguish clusters from the rest

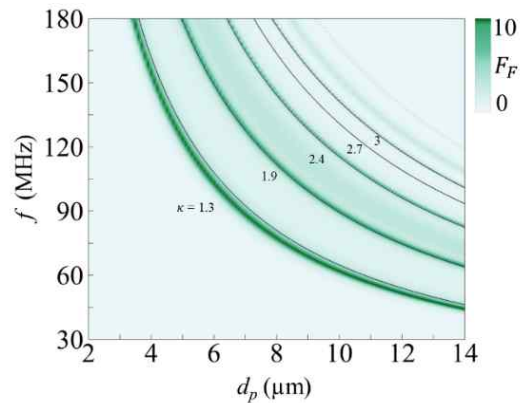


**Fig. 3.** Acoustic Radiation Force Factor ( $F_F$ ) plot with varying frequency ( $f$ ) and diameter ( $d_p$ ) of the *S. cerevisiae*.

of the shapes, while subsequent separation was deliberate to distinguish doublets from singlets. Using this theoretical estimation as a foundation, we employed frequencies of 100 MHz and 141 MHz to simultaneously manipulate the clusters and doublets, respectively, through the ARF induced by TSAWs.

### 3. Result and Discussion

Fig. 4 demonstrates the acoustofluidic separation of *S. cerevisiae* cells upon experiencing TSAW-induced ARF when frequency and acoustic power of 100 MHz and 109 mW, respectively. The solution containing three categories of *S. cerevisiae* cells mixture was injected into the central inlet with a flow rate of 10  $\mu\text{L/h}$ . The solution containing 0.1% (w/v) of *S. cerevisiae* cells was mixed in deionized water. The sheath fluid flow rate was finely tuned to direct cells toward the bottom wall of the microchannel in the acoustic assessment zone. The flow rates of sheath fluids at inlet 1 and

inlet 3 were 10  $\mu\text{L/h}$ , and 50  $\mu\text{L/h}$ , respectively. Flowrates at the inlets were carefully chosen in order to align cells flowing in the main acoustic deflection zone towards the bottom wall of the microchannel. The selected flow rates at the inlet ensure the single trajectory of cells in the main acoustic deflection zone. The fine-tuning of sheath fluid flow rates played a fundamental role in guiding cells precisely toward the bottom wall of the microchannel within the designated acoustic assessment zone. By directing cells along a clear, single path and positioning them close to the lower wall of microchannel, the experiment aimed to enhance the clarity and precision of cell observations during their interaction with TSAW. Lastly, the flow rates of sheath fluids served the additional purpose of preventing the formation of the MAC region. This region, characterized by a weak acoustic field, emerges within the channel due to the propagation of a leaky acoustic wave at the Rayleigh angle. The speed of cells flowing in the device could be easily controlled by the

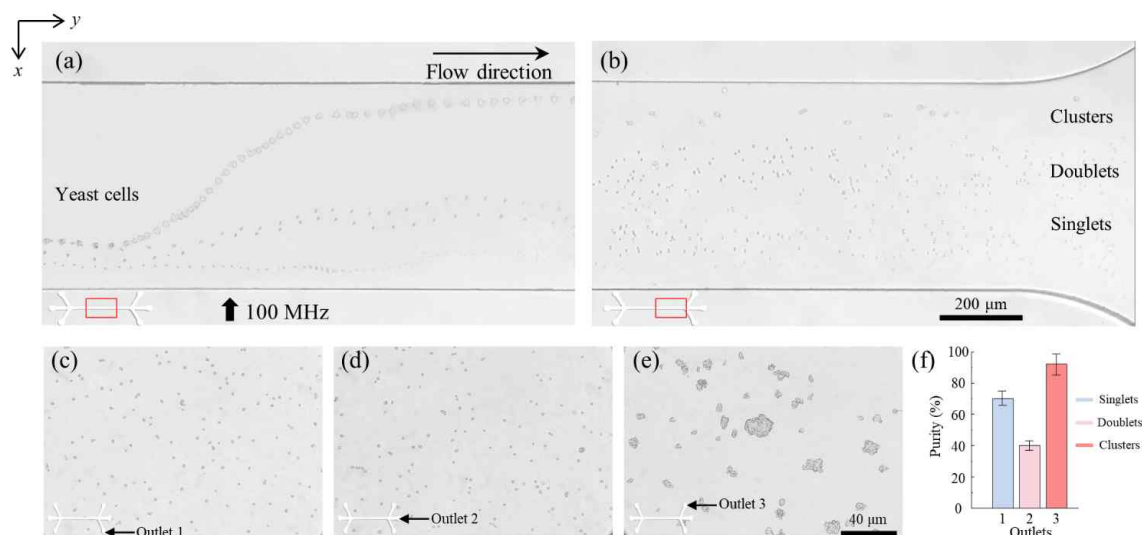


**Fig. 4.** (a) and (b) Experimental stacked microscopy images of the first separation of clusters from singlets and doublets at frequency of 100 MHz and acoustic power of 109 mW. The clusters have greater deflection distances than singlets and doublets; (c) Microscopy images of collected cells at outlet 1; (d) Microscopy images of collected cells at outlet 2; (e) Microscopy images of collected cells at outlet 3; (f) Purity of singlets, doublets, and clusters at each outlet.

volumetric flow rates of the inlets. In all the performed experiments, flow rates were kept constant in order to compare results more effectively. Fig. 4(a) shows the different trajectories of singlets, doublets, and clusters when they experienced an acoustic wave. Without the application of TSAW, cells flow toward the outlet undeflected. When acoustic power of 109 mW and frequency of 100 MHz was applied, the SFIT resonated, and traveling surface acoustic waves were produced. As the size of the yeast cells increased, the deflection distance of the cells was measured to be linearly increased. Clusters were pushed farther as a result of experiencing ARF, followed by doublets and singlets. This phenomenon can be attributed to the increased portion of wave scattering when cell size was increased, leading to a higher magnitude of ARF. At the working frequency of 100 MHz, the  $\kappa$  values were calculated as 0.573, 0.976, and 2.779 for singlets, doublets, and clusters, respectively. Fig. 4(c-e) shows the microscopic images of separated singlets, doublets, and clusters collected from Outlet 1, Outlet 2, and Outlet 3, respectively. Fig. 4(f) shows the purity of collected cells at the outlets. The purity is calculated as the ratio of one-shaped amount of yeast cells at the outlet to

the total number of yeast cells containing all shapes at the inlet. The purity of clusters at Outlet 3 was reported to be over 92% higher than the other cells. Singlets and doublets purities were 85% and 40% at Outlet 1 and Outlet 2, respectively.

We further extended our work to separate the collected singlets and doublets from outlets 2 and 3 to enhance the purity further. In the first separation experiment, the primary objective was to selectively separate clusters, collecting singlets and doublets for subsequent separation processes. When a frequency of 100 MHz was applied, the clusters experienced an enhanced magnitude of ARF in comparison to singlets and doublets. Resultingly, the purity of clusters is maximum flowed by singlets and doublets. The reduced purity of doublets observed in this stage can be attributed to the substantial size variability present within both singlets and doublets. Therefore, subsequent separation was realized to separate the doublets and singlets. Furthermore, if the parameter  $\kappa$  is less than zero ( $\kappa < 0$ ), the influence of acoustic streaming flow tends to dominate over ARF in yeast cell manipulations<sup>(13,16)</sup>. This dominance of acoustic streaming flow in cases where  $\kappa$  is less than zero results in a reduction in separation

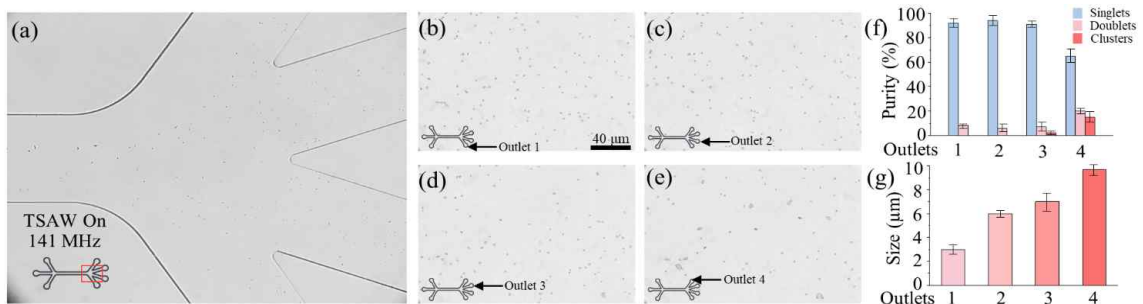


**Fig. 5.** (a) Experimental stacked microscopy images of the second separation of singlets and doublets at frequency of 141 MHz and acoustic power of 120 mW. Doublets with larger effective diameter ( $d_p$ ) deflect greater than singlets having a smaller  $d_p$ ; (b) Microscopy images of collected cells at outlet 1; (c) Microscopy images of collected cells at outlet 2; (d) Microscopy images of collected cells at outlet 3; (e) Microscopy images of collected cells at outlet 4; (f) Purity percentage of *S. cerevisiae* in each outlet; (g) Size distribution of *S. cerevisiae* in each outlet.

efficiency. In the second separation experiment, a meticulous approach was adopted to optimize the separation of doublets. In order to target only doublets from the mix population of singlets and doublets, the selection of an effective frequency corresponding to their average size was made, as illustrated in Fig. 3. This deliberate choice aimed to enhance the precision of the separation process ensuring an effective isolation of singlets and doublets. The collected cells from the previous separation were flowed through the microchannel at a flow rate of 20  $\mu\text{L/h}$  and exposed to the ARF as shown in Fig. 5. The flow rates of inlet 1 and inlet 3 were 20  $\mu\text{L/h}$ , and 200  $\mu\text{L/h}$ , respectively. Fig. 5(a) shows the different trajectories of singlets and doublets when they experienced an acoustic wave. In this experiment, the effective frequency of TSAWs was chosen as 141 MHz to separate the doublets from singlets effectively. At the working frequency, the  $\kappa$  values were calculated as 0.808 and 1.376 for singlets, and doublets, respectively. The device utilized for this experiment consists of four outlets. When acoustic power of 120 mW was applied across the terminal of the second SFIT, traveling surface acoustic waves were produced and interacted with the cells flowing in the perpendicular direction. The doublet cells were seen to be deflected since they experienced an enhanced magnitude of ARF as compared to singlets. The cells were separated and collected at the outlets as depicted in Fig. 5(b-e). Each outlet indicated a high purity of singlets with over 65% (Fig. 5(f-g)). On the other hand, doublets were primarily separated through outlet 4 with a 20% purity.

#### 4. Conclusion

This study presents a novel acoustofluidic method to separate *S. cerevisiae* cells according to their sizes. The separation relies on the application of surface acoustic waves TSAW-induced ARF. To

achieve this, we employed a cross-type microfluidic device where the TSAWs propagated perpendicular to the fluid flow direction, interacting with *S. cerevisiae* cells and exerting an ARF. By utilizing the ARF induced by TSAWs on cells of diverse sizes, we effectively accomplished the size-based separation of *S. cerevisiae* cells. This study involves a two-step separation using two devices comprises of two SFITs to separate singlets, doublets, and clusters with high purity. The first separation was done at 100 MHz to separate clusters from other cells, giving it the highest purity of 85% compared to other cells. The extended separation by 141 MHz frequency was aimed at the enhancement of the purity of these cell populations and ensuring the reliability and stability of the separation device. A purity of 95% was singletons. However, the purity of doublets was limited to 20%.

#### Acknowledgements

This work was financially supported by Chonnam National University (Grant number: 2023-1161-01) and the National Research Foundation of Korea (NRF) grant funded by the Korea government (MSIT) (No. RS-2023-00210891). The microfluidic devices were fabricated by using a mask aligner (MDA-400S, MIDAS) at Energy Convergence Core Facility in Chonnam National University.

#### REFERENCE

- 1) Nathalie B., Sarah R., Hugo R., Fanny G., Pascal V., Mickael B., Mickael D., 2023, "*Saccharomyces cerevisiae*: Multifaceted Applications in One Health and the Achievement of Sustainable Development Goals.", *Encyclopedia*, Vol. 3(2), pp.602~613.
- 2) Maria P., Anastasios V., Amalia-Sofia., Efstathios H., 2020, "*Saccharomyces cerevisiae* and Its Industrial Applications.", *Microbiology*, Vol. 6

- (1), pp.1~31.
- 3) Elena I. S., Sergey P. Z., Andrey R. S., Anna Y. A., 2023, "Practical Approaches for the Yeast *Saccharomyces cerevisiae* Genome Modification.", *International Journal of Molecular Sciences*, Vol 24(15). pp.1~33.
  - 4) Sideney B. O., Ivan C. B., Dirceu A., Douglas R., 2017, "Chemical Composition of the Biomass of *Saccharomyces cerevisiae* - (Meyen ex E. C. Hansen, 1883) Yeast Obtained From the Beer Manufacturing Process.", *International Journal of Environment, Agriculture, and Biotechnology (IJEAB)*, Vol. 2, pp. 558~562.
  - 5) Aashiq H. K., Michelle V., Brittany M. G., Mudabir A., 2022, "Humanized Yeast to Model Human Biology, Disease, and Evolution.", *Dis Model Mech.* Vol. 15(6), pp.1~13.
  - 6) Ping L., Hangrui L., Dan Y., Daniel J., Sheng Y., Ming L., 2021, "Separation and Enrichment of Yeast *Saccharomyces cerevisiae* by Shape Using Viscoelastic Microfluidics.", *Analytical Chemistry*, Vol. 93(3), pp.1586~1595.
  - 7) Matthew J. T., Sophie T., Xuebin B.Y., Jennifer K., 2012, "Cell Separation: Terminology and Practical Considerations.", *Journal of Tissue Engineering*, Vol. 4, pp.1~14.
  - 8) Muthusarayanan S., Ram K., Deenadayalan K.G., Yogesan M., Kumaravel K., 2020., "Active Microfluidic Systems for Cell Sorting and Separation.", *Current Opinion in Biomedical Engineering*, Vol. 13, pp.60~68.
  - 9) Yueyue Z., Tingting Z., Li W., Liang F., Min W., Zhenchao Z., Huanhuan F., 2021., "From Passive to Active Sorting in Microfluidics: A Review.", *Rev. Adv. Mater. Sci*, Vol.60, pp.313~324.
  - 10) Eliezer K., Ayelet C. A., Aaron C., Alexander I. A., Reshef M., Merav C., Dana R., Daniel K., Yaakov N., 2018, "High-Reynolds Microfluidic Sorting of Large Yeast Populations.", *Scientific Reports*, Vol 8(1), pp.1~13.
  - 11) Honeyeh M. E., Christian W., 2021, "Characterization and Separation of Live and Dead Yeast Cells Using CMOS-Based DEP Microfluidics.", Vol. 12(270), pp.1~19.
  - 12) Muhammad A., Jinsoo P., Ghulam D., Husnain A., Syed A. I., Sanghee K., Sunghyun K., Anas A., Tae-Sung Y., Hyung J. S., 2020, "Acoustomicrofluidic Separation of Tardigrades from Raw Cultures for Sample Preparation.", Vol. 188(3), pp.809~819.
  - 13) Ghulam D., Byung H.H., Jinsoo P., Jin H.J., Anas A., Hyung J. S., 2015, "Microchannel Anechoic Corner for Size-Selective Separation and Medium Exchange via Traveling Surface Acoustic Waves.", *Analytical Chemistry*, Vol 87(9), pp.4627~4632.
  - 14) Muhammad S. K., Mehmet A. S., Ghulam D., Jinsoo P., 2022, "Residue-Free Acoustofluidic Manipulation of Microparticles via Removal of Microchannel Anechoic Corner.", *Ultrasonics Sonochemistry*, Vol. 89, pp.1~10.
  - 15) Mushtaq A., Beomseok C., Muhammad S. K., Hyunwoo J., Song H. L., Woohyuk K., Jeongu K., Jinsoo P., 2022, "Size-Based Separation of Microscale Droplets by Surface Acoustic Wave-Induced Acoustic Radiation Force.", *Journal of the Korean Society of Visualization*, Vol. 20(3), pp.19~26.
  - 16) Mehmet A.S., Mushtaq A., Jinsoo P., Ghulam D., 2023, "Fundamentals of Acoustic Wave Generation and Propagation.", *Acoustic Technologies in Biology and Medicine, First Edition*, pp.1~36.
  - 17) Takahi H., Yosioka K., 1969., "Acoustic-Radiation Force on a Solid Elastic Sphere.", *The Journal of the Acoustical Society of America*, Vol. 46, pp.1139~1143.
  - 18) Husnain A., Ghulam D., Ashar A., Kwangseok P., Jinsoo P., Jin H. J., Hyung J. S., 2017, "A Pumpless Acoustomicrofluidic Stage for the Size-Selective Concentration and Separation of Microparticles.", *Analytical Chemistry*, Vol. 89, pp.13575~13581.